Investigation on the characterization of hot extruded AA7075 based metal matrix composites developed by powder metallurgy

Investigation on the characterization of hot extruded AA7075 based metal matrix composites developed by powder metallurgy

Babu B[1], Meinathan S[2], Manikandan P[3], Lingeswaran P[4], Nanthakumar S[5], Yasminebegum A[6], Girimurugan R[7*]

[1]Department of Mechanical Engineering, Amrita College of Engineering and Technology, Nagarcoil 629 901, Tamilnadu, India

[2]Department of Mechanical Engineering, Shree Venkateshwara Hi-Tech Engineering College, Erode 638 455, Tamilnadu, India

[3]Department of Mechanical Engineering, K S R Institute for Engineering and Technology, Tiruchengode 637 215, Tamilnadu, India

[4]Department of Mechanical Engineering, Shree Venkateshwara Hi-Tech Engineering College, Erode 638 455, Tamilnadu, India

[5]Department of Mechanical Engineering, PSG Institute of Technology and Applied Research, Coimbatore 641 062, Tamilnadu, India

[6]Department of Electronics and Instrumentation Engineering, Sree Vidyanikethan Engineering College, Tirupati 517 102, Andhra Pradesh, India

[7]Department of Mechanical Engineering, Nandha College of Technology, Perundurai 638 052, Tamilnadu, India

Abstract. Higher compressive stress and greater density after extrusion contribute to stronger bonds, which in turn improves mechanical and tribological properties were analyzed. In order to minimize manufacturing defects, a cosine-profiled die with mathematically precise contours was used in the thermo mechanical process. It was requested that more mechanical characterization tests, such as a compression testing and a three-point bending test, be directed to better define the material's density, hardness, and ductility. Before and after extrusion, the prepared AMCs were put through pin-on-disc (POD) wear testing, during which the RPM of the counter disc, load (N) and track diameter (mm) were varied to simulate different two-body dry sliding wear behaviors. Hot extrusion of AA7075 aluminium matrix composites (AMCs) was investigated for its effect on the materials' mechanical and tribological properties. These AMCs were manufactured by controlled atmospheric sintering, powder metallurgy and double axial cold compaction. The finely dispersed graphite (Gr) particles shear off at the tribo-surface, creating a solid lubricant that slows the rate of wear. The wear mechanism was found to be more complex when the loading and sliding velocities were increased.

Keywords: hot extruded, powder metallurgy, load, track diameter, metal matrix composites, wear mechanism.

1. Introduction

There has been a lot of study into the improvement of powder metallurgy (P/M) pathway developed Al-based MMCs during the past few decades [1]. A few of the main benefits of this type of production include the uniform dispersal of strengthening particles, the use of minimum temperatures, and the capacity to create near net form products of complicated pattern [2-4]. There have been multiple investigations into the impact of reinforcing very hard metals and ceramics in varying alumina powder matrices [5-6]. Sintering causes layers of oxide to grow in the powder metallurgy specimen because aluminium is so easily oxidized. Evidence for a larger relative velocity variation at the die exit, which occurs during thermo-mechanical treatments, leads to product flaws due to a sturdily bonded microstructure and a better facing die in extrusion [7-8]. For optimal results when extruding MMC, it's best to use a die with a mathematically contoured shape [9]. Researchers [10] looked at how changing the graphite content, stress, relative velocity, and sliding distance affected the wear behavior of a P/M composite made from aluminium. In order to improve wear resistance, fine graphite reinforcing is used to compromise hardness, flexural strength, fracture toughness [11-12]. Hot extrudability is enhanced by the inclusion of zinc with aluminium, but high-temperature performance is diminished. Given these considerations, a smaller percentage of the total weight of the reinforcements was retained for this operation [13]. The marginal increase in wear rate owing to an increasing quantity of TiC can be predicted to be significantly different from the linear relationship between applied load and wear rate [14-15]. The mechanical characteristics of the aluminium alloy reinforced with fly ash were studied by researchers [16]. More reinforcement can be added, sacrificing some ductility in exchange for improved mechanical qualities [17]. In this study, authors analyze the tribo-mechanical properties of AMCs that was synthesized by an extrusion process using a powder metallurgy synthesis technique. AA7075 + Mg + Gr matrix with two different metal reinforcements, zinc, and titanium, was added so that the two combinations could be compared. Investigations were made into the qualities of AMCs before and after they were subjected to a thermal mechanical treatment using a cosine die with a geometrically curved profile.

2. Methods

2.1 Sample Preparation

For the matrix, a mixture of aluminium AA7075 (92.33%), magnesium (4.26%), and graphite (0.85%) was used. Zn and Ti were both added to the mixture as reinforcements to make two distinct test specimens. Table 1 lists the constituent parts of two samples. Powders' size, shape, and flowability, among other physical properties, were investigated.

Table 1. Detailed composition

Sample	Composition
1	AA7075 (97.76) + Mg (0.8) + Gr (0.85) + Zn (6.1)
2	AA7075 (97.76) + Mg (0.8) + Gr (0.85) + 1.70 Ti

Authors used a centrifugal blender to blending of the ingredients. The proportion of SS steel ball to powder was always 10 to 1. For 10 hours, the mixture was blended at 250rpm. Authors evaluated the powders' flow properties by measuring their apparent density and tap density after they had been blended. To create the green pellets, authors first compressed the powder in two directions, at perpendicular to one another. For the compaction process to work, the powder inside the container must remain in a free-flowing state between the two punches. Over the course of 10 minutes, the precipitate was exposed to a pressure of 285 MPa, which gradually increased. Green density was measured for the prepared pellets, which had a diameter of 10 mm. Sintering of green pellets was performed in a tubular furnace with a controlled environment of argon [18]. Each increment of 5°C/min in temperature was set. Water vapor was removed during a 20 minutes

dwell at 120 °C, zinc stearate was burned off during a 30 minutes dwell at 450 °C, and the metallic bond was formed during a 90 minutes dwell at 590 °C.

2.2 Secondary Processing

A pellet with a diameter of 10 mm was cold compacted and sintered, and then hot extruded as a subsequent processing step. To achieve a 50% reduction in pellet cross section, tests were conducted at 400°C -450 °C operating temperature and 3mm/min ram rate. Significant surface defects, like surface fractures and rips, are introduced into the extruded product during shear-faced die extrusion because of the relative difference in velocities at the die exit[19]. When making MMCs through the powder metallurgy process, extrusion is a more likely scenario to cause faults. When transitioning from extruding rounds to square bars, a cosine die was employed to minimize the impact of the speed differential between the two processes. In Fig. 1, authors see a 2D drawing of the extrusion tooling setup along with the coordinates of a generated profile in one of the four cardinal directions.

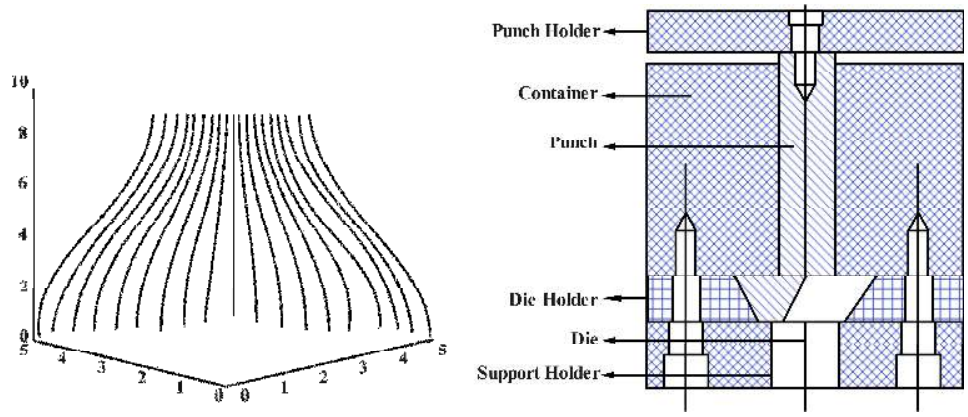

Figure 1. (a) The cosine die's one-quadrant profile's profile coordinates. (b) 2D cad drawings of the equipment configuration

2.3 Tribological and Mechanical properties

Densities such as theoretical, green, sintered, and extruded were examined from other manufacturing processes. Measurements of theoretical density were made using the formula in Eq. 1. [20]

$$\rho_{\text{Theoretical}} = \sum(\rho_{\text{i}} \times m_{\text{i}}) \quad (1)$$

Archimedes' principle was used to determine the densities of both solid-sintered and extruded pellets. The formula for determining density is given in eqn (2) [21-23].

$$\rho_{\text{sample}} = \frac{W_{\text{A}} \times \rho_{\text{fluid}}}{W_{\text{A}} - W_{\text{fluid}}} \quad (2)$$

The Vickers micro-hardness of sintered MMC composites was evaluated by dividing the applied force by the area that was impressed. Authors placed a 60g load over a pyramid(diamond) with an angle of 141° for 20s to eliminate any possible spring back effects. The Transverse Rupture strength (TRS) of sintered solid cylindrical specimen was determined by performing a three-point bend test. As can be seen in Fig. 2, the test was conducted on a universal testing machine (UTM; Instron model -5979). At room temperature, the compression rate was 4 mm/min while the span remained constant at 40 mm.

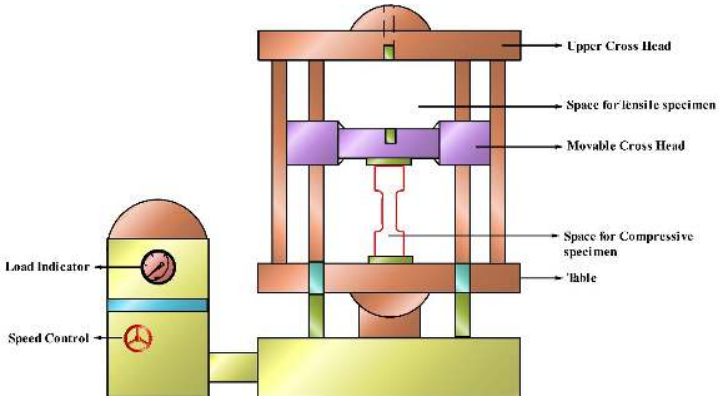

Figure 2. A Schematic diagram of universal testing machine

2.4 Testing of Wear

Pin-on-disc wear testing equipment was used to investigate the aluminium MMC's resistance to wear under dry sliding conditions. The pins, which measured around 10mm in diameter and 25mm in length, were given a flat contact surface and rounded corners before being put in a sample holder at right angles to the counter disc. For this experiment, authors used a counter body consisting of a spinning disc made of EN-31, which had a hardness of 60HV and a surface roughness (Ra) of 2 µm. The acetone used to clean the pin surface and the counter disc for this experiment. A lever attachment on the specimen holder was used to exert a standard force on the MMC particle. In Fig. 3 authors see a schematic view of the process used to test for wear. Machine setup allows for easily adjustable variables such as track diameter, normal load, and disc rpm; however, these parameters must be established to set before any testing can begin. Table 2 lists the variables and factors used in the wear analysis. Each experiment was designed to last for 10 minutes. The wear loss was calculated by comparing the initial and final masses of the MMC pin (sample), with an accuracy of 0.1 mg.

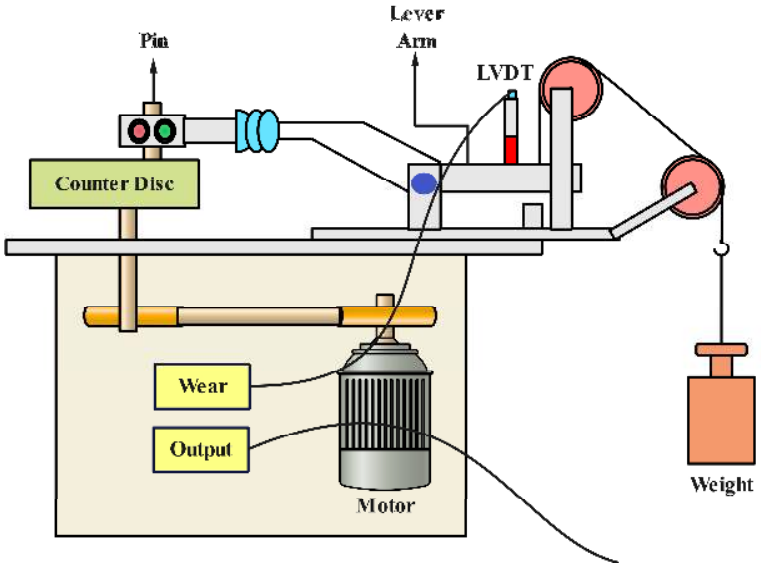

Figure 3. A schematic arrangement of pin-on-disc wear test

Table 2. Selecting experimental factor Variables

Variable factor	Units	Level		
		1	2	3
RPM of counter disc	(N)	250	500	750
Normal load (L)	(N)	30	60	90
Wear track diameter (D)	(mm)	60	80	100

3. Results and discussions

3.1Physical properties

Physical qualities and environmental factors have a direct impact on the powder's flowability[24]. There is a close relationship between the product's flowability and its mechanical and tribological properties. Understanding the particles' sizes, shapes, and densities through scientific research is so crucial. For this purpose, authors used microscopy and image analysis, but this research investigated laser diffraction and sieve analysis, two more common techniques for determining particle size and shape. Particle size and shape of Powders were analyzed using image analysis software. Table 3 shows the comprehensive results.

Table 3. Physical properties of different powders

Powder	Average size (μm)	Dimension of particle	Purity/assay (%)
Al	48	Rounded and slightly spherical	97.0
Mg	1405	Flakey	98.0
Gr	22	Flaky and rounded	97.0
Zn	25	Rounded and slightly spherical	97.0
Ti	88	Extremely angular and irregular	97.0

3.2Investigation of Density

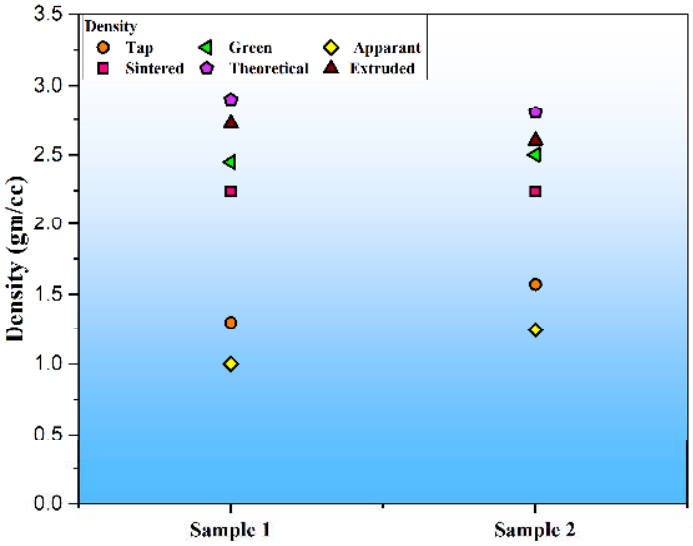

Figure 4. Density plot

Both the apparent/bulk and tap densities were measured directly. Figure 4 shows that tapping the blended powder results in a 40-45% increase in density. Compaction pressure is the primary factor in determining the pellet's green density. Even in the green specimens, good consolidation of metallic particles was seen at 285 MPa. After precisely measuring both the volume and mass, authors were able to determine the density by dividing the former by the latter (with the accuracy of 0.001 g). Eq. 3 depicts the relation used to determine the non-dimensional densification parameters[25], [26].

$$\text{Densification factor} = \frac{(\text{sintered density-green density})}{(\text{theoretical density-green density})} \tag{3}$$

For densification parameters, a positive value indicates a reduction in volume, whereas a negative value suggests an increase. Now of sintering, all the samples are exhibiting swelling behavior. Eq. 4 shows the relation that can be used to determine the percentage densification improvement brought about by thermo-mechanical treatment (extrusion) [27].

$$\text{Percentage Enhancement on densification} = \frac{\text{extruded density - sintered density}}{\text{sintered density}} \tag{4}$$

Figure 4 shows that the density has increased by 20-25% after extrusion, with a corresponding reduction of 50%. Table 4 displays the computed densification factors, density increases, and porosities. Type 1 sample is denser than type 2 because of a greater concentration of zinc.

Table 4. Analysis of porosity

Specimen	Specimen 1	Specimen 2
Densification parameter	−0.612	−0.823
Percentage enhancement on densification (after extrusion)	21.46	18.24
Porosity before extrusion (%)	24.9	23
Porosity after extrusion (%)	9.56	9.62

3.3 Mechanical analysis of a sintered specimen subjected to compression

At room temperature, a UTM (Instron-setec series) was used to compress all pellet types at a rate of 3 mm/min. Figure 5 (a) and (b) depicts the relationship between output stress and strain. Collectively, the ultimate strength of the two specimen is 412 MPa for sample 1 and 393 MPa for sample 2. Type 1 specimens have superior strength because of the strong bond strength produced by liquid phase sintering.

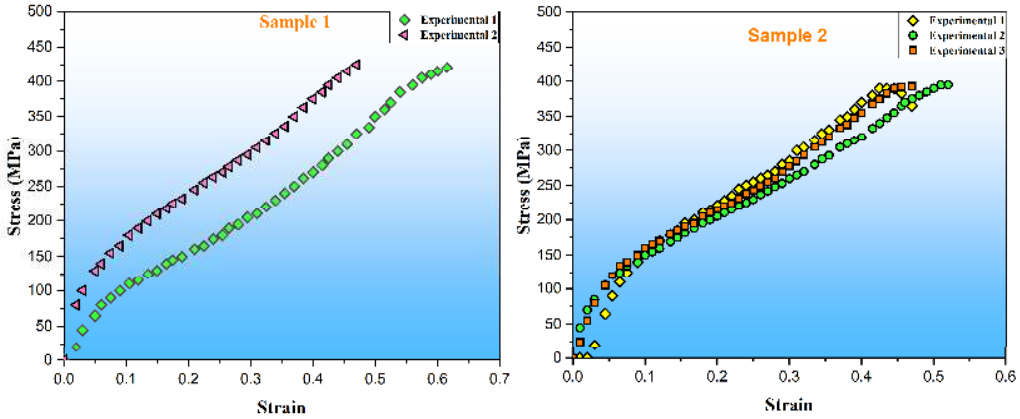

Figure 5. A curvature of Stress vs strain (a) sample 1 and (b) sample 2

3.4 Evaluation of Micro-hardness

Ten measurements were taken of sintered and extruded products, and the mean micro-hardness was derived from these values. Figure 6a demonstrates that the material's hardness is enhanced by 35-40% following extrusion after being manufactured using the method. In addition to the mismatch in mechanical properties and temperature, a greater dislocation density can be found around the reinforcing particles. Increased mechanical properties are the result of the accumulation of huge amounts of internal and thermal stress caused by the mismatch in characteristics between the matrix and reinforcements.

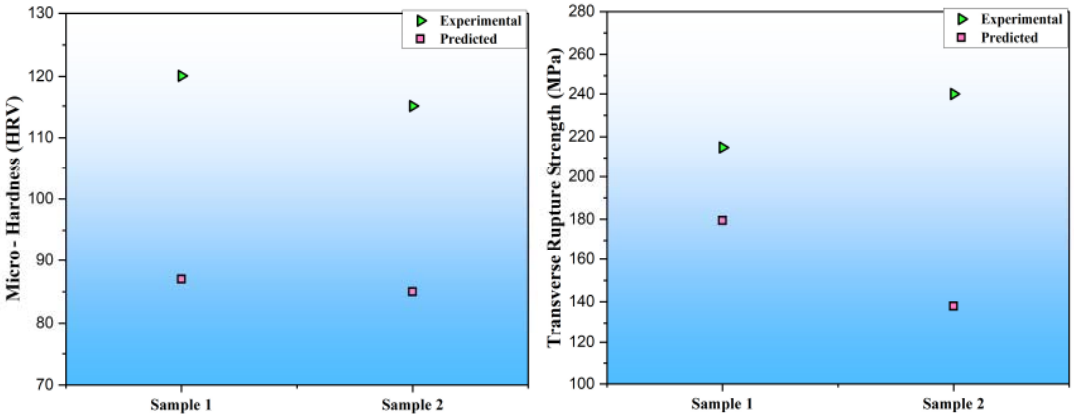

Figure 6. Comparison of experimented and predicted results of (a) Transverse rupture strength and (b) Micro-hardness

3.5 Three-point bending test

For both sintered and extruded specimens, the TRS in MPa was determined by utilizing the relations provided in equations 5 and 6.

$$\text{Tansverse Rupture strength} = 8Pl/\Pi D^3 \quad (5)$$

$$\text{Tansverse Rupture strength} = 3Pl/2d^3 \quad (6)$$

In Fig. 6 (b), the typical TRS of every sintered and extruded sample taken together was shown. Type 1 sample sintering occurred in the liquid phase at 600°C because of zinc, which has a melting point of 420°C, was present. Ti-reinforced samples had a lower probability of fracture formation than TRS due to the existence of a high-stress concentration at the boundary zone of the reinforcements.

3.6 Wear test

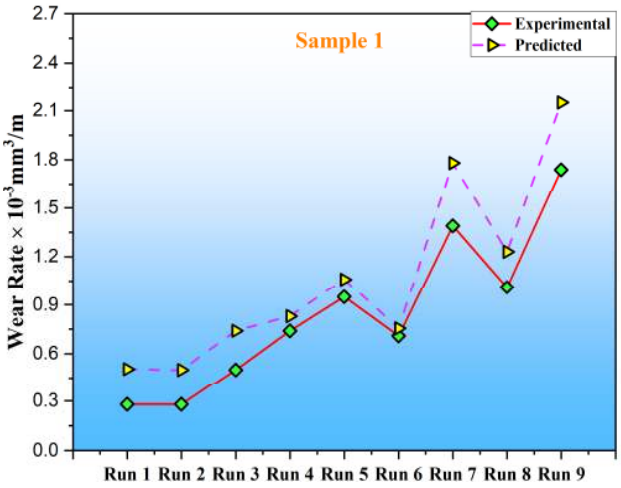

Figure 7. Comparison of wear rate for every trial for sample 1

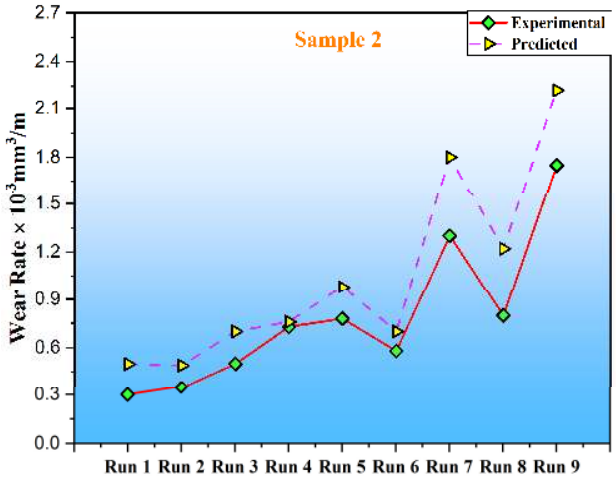

Figure 8. Comparison of wear rate for every trial for sample 2

Table 5. Design of Experiments for wear testing

Run	Load	Track diameter	RPM of counter disc
1	30	60	250
2	30	80	500
3	30	100	750
4	60	60	500
5	60	80	750
6	60	100	250
7	90	60	750
8	90	80	250
9	90	100	500

When evaluating extruded and sintered samples, an orthogonal array (Table 5) was designed, with each of the three variables having three levels. Figures 7 and 8 show the range of wear rates for sintered and extruded specimens of two composite respectively. Authors calculated the mass loss of pin by comparing the pre- and post-wear mass readings of the sample. As for the test definition of mass loss as follows:

$$\Delta w = (w_{\mathrm{a}} - w_{\mathrm{b}}) \tag{7}$$

The following relation is used to approximate the AMCs' volume loss:

$$\text{Volume loss} = \frac{\text{Mass loss}}{\text{Density}} \tag{8}$$

Using the relation, authors were able to calculate the wear rate Wr in terms of volume.

$$Wr = \frac{\text{Volume loss}}{\text{Sliding distance}} \tag{9}$$

Numerous studies have shown a direct correlation between hardness and durability. Extrusion strengthens the matrix's link to the reinforcement material, which in turn increases the material's resilience to wear and eliminates the possibility of three-body abrasive wear.

3.7 Wear microscopy

The depth of grooving in extruded specimens is less than that in AMCs. Groove linings of the unextruded AMCs show severe plastic deformation and have a coarse texture. There is also debris in the form of granules and flakes around the divots. When the load is 40N or 60 N and the rotational speed is 600 rpm, grooving and scratching are more important than abrasion. Images reveal a significant number of white particles at the tribo-surface, the result of oxidation of the surface brought on by frictional heating. The delamination and combined abrasion, delamination, and adhesion wear mechanisms become apparent under extreme loading and velocity conditions. Subsurface crack formed by fatigue failure of the pin caused by repeated sliding behavior. Long-distance propagation of these subsurface fissures results in surface shear deformation. Plastic deformation is primarily caused by melting, thermal softening, and adhesion under unfavorable conditions. The wear mechanism of AMCs is milder compared to that of base metal alloys [28]. Sheared graphite particles in a metal/Gr composite form a lubrication layer on the tribo-surface, reducing friction and wear by preventing the metals from coming into direct contact.

4. Conclusions

Extrusion's influence on the enhancement of the AMCs' mechanical and tribological characteristics was studied. The following is a summary of the findings from these studies: By increasing the bond strength during the extrusion process, the mechanical qualities of all types of aluminium matrix composites are enhanced. Supporting the enhancement of flexural strength and tribological qualities, the extruded product was discovered to have a remarkably low number of surface defects. After each run, the extruded specimen shows less wear than the sintered one. Liquid phase sintering results from the inclusion of zinc due to its low melting temperature, which results in increased bond strength and density and improved performance. If the heat conductivity can be sacrificed, adding more fine titanium could vastly increase the characteristics. Cropping of the uniformly dispersed Gr particles at the tribo-surface creates lubrication. Therefore, the wear resistance is enhanced by adding Gr particle while only a small quantity of hardness is lost. Wear mechanisms such as oxidation, delamination, adhesion, and abrasion all work together under conditions of increased stress and sliding velocity. A closer look reveals that oxidative and delamination wear are the surface's dominant wear mechanisms. These composites can be used in aerospace applications.

References

[1] Jagannatham M *et al.,* 2018 *J Mater Eng Perform* **27** 5675.

[2] Baskaran S *et al.,* 2014 *Applied Mechanics and Materials* **541** 263.

[3] B. Ramesh *et al.,* 2022 *J Nanomater*.

[4] Estrada-Ruiz R H et al., 2022 *Adv Powder Technol* **33.**

[5] Ngernbamrung S *et al.,* 2018 *Procedia Manufacturing* **15** 217.

[6] Kamble, A G *et al.,* 2022 *J Inst Eng Ser D*.

[7] Manohar G, *et al.,* 2020 *Journal of Physics: Conference Series* **1451**.

[8] Xu R *et al.,* 2018 *Compos Part A Appl Sci Manuf* **111** 1.

[9] Keerthivasan N et al., 2022 *Part Sci Technol*.

[10] Kishore K L et al., 2022 *Mater Today Proc* **62** 4424.

[11] Enginsoy H M 2018 *et al., Compos Part B Eng* **162** 397.

[12] Kumar S 2008 *et al., Wear* **264** 1026.

[13] Salmaan N U *et al.,* 2022 *Int J Interact Des Manuf*.

[14] Feijoo I *et al.,* 2021*Metals (Basel)* **11**.

[15] Manohar G *et al.,* 2020 *Materials Today: Proceedings* **45** 6321.

[16] Durmuş H *et al.,* 2020 *Sci Sinter* **52** 177.

[17] Chinnaiyan S *et al.,* 2018 *Mater Tehnol*, **52** 809.

[18] Sahoo G *et al.,* 2022 *Materials Today: Proceedings* **56** 3201

[19] Girimurugan R *et al.,* 2021 Int J Mech Eng **6** 1073.

[20] Saravanan C *et al.,* 2018 *Ind Lubr Tribol* **70** 1066.

[21] Manohar G et al., 2022 *Silicon* **14** 7831.

[22] Manohar G *et al.,* 2021 *Lecture Notes in Mechanical Engineering* 343.

[23] Gandhi C, *et al.,* 2019 *Materials Today: Proceedings* **18** 37

[24] Aydin F *et al.,* 2021 *Adv Powder Technol* 32 445.

[25] Wu J *et al.*, 2021 *Mater Sci Eng A* 825.

[26] Feijoo I *et al., Metals (Basel)* 12.

[27] Enginsoy H M *et al.,* 2020 *Compos Part B Eng* 194.

[28] Vairavel, M *et al.,* 2020 *In AIP Conference Proceedings*, **2283** 020112.